GEOSPATIAL DIMENSIONS OF LAND COVER TRANSITIONS AND LAND SURFACE TEMPERATURE IN ABUJA CITY, NIGERIA

Y.M. Salmamza [1,*], S.M. Onywere [1], S.C. Letema [1]

[1] Department of Spatial and Environmental Planning, Kenyatta University, Nairobi, Kenya
smsheila@students.ku.ac.ke, (onywere.simon, letema.sammy)@ku.ac.ke

Commission III, WG III/7

KEY WORDS: Urban Heat Island, Land Surface Temperature, Land Cover, Thermal Comfort, Google Earth Engine

ABSTRACT:

Urbanization is often accompanied by succession of underlying land cover with impervious surfaces. Built intensification significantly alters the surface energy budget making cities warmer than their outlying suburbs, which signifies an ecological deterioration. Landsat imageries with scene covering Abuja city is processed using Google Earth Engine platform to estimate land cover and land surface temperature over the span of 30 years (1990-2020). Dimensions of land cover transitions were examined in-terms losses, gains, swaps, net-change and persistency. Thermal signature of each land cover type was estimated using land surface temperature. Urban thermal field variance index is computed from land surface temperature to evaluate the thermal conditions in the city. Results indicate that net-changes for built-up exhibited gains of 40% while agricultural land, bare-land and vegetation exhibited loss of 27%, 7% and 8% respectively. Built-up also showed the highest proportion of persistence (12%). Results shows that land surface temperature has increased by 2.01°C from 1990 to 2020. Agricultural land, bare-land and built-up were found with the highest temperature. Lowest temperature was found in waterbody and vegetation. The ecological evaluation showed that 47% of the city is experiencing bad to worst thermal condition. These findings provide further information that can contribute towards an informed spatial planning in cities.

1. INTRODUCTION

The worlds urban population is above 50% and projected to reach 70% by 2050 (UN-Habitat, 2019). Cognizant of the fact that 35% of the projection will come from China, India and Nigeria (UN-DESA, 2019). Urbanization is often accompanied by profound alteration of underlying natural surfaces such as vegetation (P W Mwangi et al., 2021). The natural surfaces are transformed into impervious structures such as roads and buildings (Filho et al., 2021). The prevalence of impervious surfaces modifies biophysical properties such as albedo, latent heat and conductivity, thereby creating Urban Heat Island (UHI) phenomena (Oke, 1973). Extreme heat has the potential of effecting the thermal comfort and health of urban dwellers (Cavan et al., 2014; EPA, 2016). This raises concerns for prior planning towards achieving the United-Nation's Sustainable Development Goals (SDGs) (UN-Habitat, 2020).

Urbanization have occurred on relatively small-fraction of Earth's land surface, but yet it contributes significantly to the loss of natural ecosystems (UNCCD, 2017). An informed land management strategy have great potential of ensuring a more secure and sustainable urban future (Hishe, 2021). There is need for a spatially resolved analytics of land cover and its ecological footprints. Remote Sensing and geographic information system (GIS) have been recognized as effective geospatial technologies for observing earth's surface features (Manakos et al., 2021). Geodata analytics provides adequate spatial detail needed for a sustainable spatial planning. Land surface temperature (LST) is a key indicator of Earth's surface energy balance (Dissanayake, 2019).

In-depth analysis of cross-tabulation matrix of land cover change provides insights on the components of transitions (Adugna et al., 2017; Pontius et al., 2004). UHI intensity is extricable linked to the anomalous changes in LST and can be ecologically evaluated using the Urban Thermal Field Variance Index (UTFVI) (Alcantara et al., 2019). Abuja City has significantly urbanized since its inauguration as the capital of Nigeria (Gumel et al., 2020). This paper aims to explore the geospatial dimensions of land cover transitions and Land Surface Temperature (LST) in Abuja city, Nigeria. The specific objectives of this study are: (I) to analyse the dynamics of land cover in Abuja City, Nigeria; (II) to analyse the pattern of LST in relation to land cover changes; and (III) to evaluate the thermal comfort of Abuja City, Nigeria.

2. METHODOLOGY

2.1 Study Area

The study focuses on Abuja City, Federal Capital Territory (FCT) of Nigeria (Figure 1). The area covers 256 km^2 and extends between latitude 7° 25' & 9° 20' Northing of the Equator and longitude 5° 45' & 7° 39' Easting of the Greenwich Meridians.

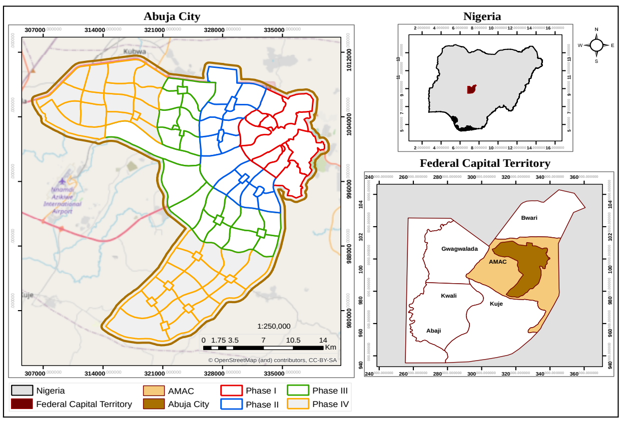

Figure 1: The Location of Abuja City, Nigeria
© Open Street Map Image Copyright 2021

Abuja City serves as the administrative and political headquarters for the Federal Government of Nigeria (FGN) (Abubakar, 2014). The area has two distinct seasons, rainy and dry. The rainy season starts in April and retreats by September, while the dry season starts in November and retreats by March (Adeyeri et al., 2017). The mean temperature ranges between 21°C and 40°C.

* Corresponding Author

2.2 Data and Pre-processing

Land cover and land surface temperature data (path:189, row:54) are excavated from Landsat collections in the GEE platform (https://earthengine.google.org/). The acquired scenes are cloud free level_1 tier (L_1T) products generated at medium resolution for 1990, 2001, 2014 and 2020 (Table 1). The images were selected within dry season to avoid phenological variability between time points (Verbesselt et al., 2010). The boundary shapefile for Abuja City was obtained from Abuja Geographical Information System (AGIS). The reference layer for training and validation is available in Google Earth. Landsat imageries were projected to Universal Transverse Mercator (UTM) Zone 32N and georeferenced to the World Geodetic System (WGS) 1984.

Satellite	Band	Resolution	Acquisition Date
Landsat 5^{TM}	7	30 m	12 - 02 - 1990
Landsat 7^{ETM+}	9	30 m	09 - 01 - 2001
Landsat 8^{OLI}	11	30 m	05 - 01 - 2014
Landsat 8^{OLI}	11	30 m	07 - 02 - 2020

Table 1: Landsat data used in the study

GEE cloud computing infrastructure facilitates advanced processing and analysis of images (Ermida et al., 2020). The L_1T Landsat imageries are calibrated to correct radiometric and geometric distortion. Prior to image analysis an atmospheric correction is performed. The acquired raw bands were converted to top of atmosphere (TOA) reflectance and radiance from digital numbers (DN) (Cetin et al., 2008). The multispectral bands were used to obtain land cover classes and Normalized Difference Vegetation Index (NDVI). While the TIR bands were used to retrieve LST. The methodology is summarized in (Figure 2).

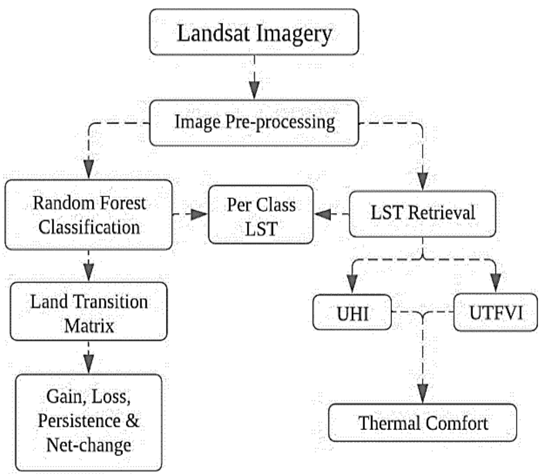

Figure 2: Flowchart of the methodology

2.3 Land Cover Classification

Random Forest (RF) algorithm was used to classify the land cover for the year 1990, 2001, 2014 and 2020. RF non-parametric image classifier yields higher accuracy amongst the other types machine leaning algorithm (Talukdar et al., 2020). The land cover classification scheme consisted of five (5) classes; agricultural land, bare-land, built-up area, vegetation and waterbody. The validation of RF classified land cover produced an overall accuracy (OA) of 82.83%, 88.64%, 90.40% and 93.76% for the years 1990, 2001, 2014 and 2020. The kappa coefficient of the reference epochs ranged between 0.80 to 0.9.

2.3.1 Post Classification Comparison

The classified images of 1990, 2001, 2014 and 2020 were over-laid to analyze the spatial dynamics of land cover. An extended two-dimensional comparison matrix of 1990 and 2020 was produced to dictate the declining, increasing and static patterns of land cover categories. The components of land cover transitions were analyzed based on losses, gains, swaps, net-change and persistency (Braimoh, 2006; Pontius et al., 2004).

2.4 Land Surface Temperature Retrieval

Statistical-Mono-Window (SMW) algorithm (Mccartney et al., 2020), was used to compute LST from the scenes of Landsat imageries for 1990, 2001, 2014 and 2020. Radiance was converted to At-sensor Brightness Temperature to rectify emissivity (ε) using Eq. (1).

$$T_\beta = K_2/1n\ (K_1/\ L_\lambda + 1) \tag{1}$$

Where,
T_β = Sensor brightness temperature (K)`
L_λ = Sensors spectral radiance (W m− 2 sr− 1 μm− 1)
K_1 & K_2 = Band specific thermal constants

The temperature was converted from degrees Kelvin to Celsius by adding an absolute 0°C (approx.-273.15°C) using Eq. (2).

$$T_\beta = K_2/1n\ (K_1/\ L_\lambda+ 1) – 273.15 \tag{2}$$

The study employed NDVI based emissivity correction using vegetation proportion (P_v) threshold method. The P_v are derived using Eq. (3).

$$P_v = (NDVI – NDVI_{soil} / NDVI_{veg} + NDVI_{soil})^2 \tag{3}$$

Where,
$NDVI_{soil}$ = Threshold values of soil pixel
$NDVI_{veg}$ = Threshold values of vegetation pixel

The calculation of land surface emissivity (ε) is crucial for the assessment of LST. It is often considered as the Plank's Law proportionality factor, which is the blackbody radiance that predicts emitted radiance. Eq. (4) is used to calculate ε_λ:

$$\varepsilon_\lambda = \varepsilon veg._\lambda\ P_v + \varepsilon soil._\lambda\ (1\text{-}P_v) + C_V \tag{4}$$

Where,
εveg.= Vegetation emissivity
Soil = Soil emissivity
C = Surface roughness

Land surface temperature is computed as expressed in Eq. (5).

$$LST = T_\beta / [1 + \{(_\lambda \cdot T_\beta/ \rho)\ In \cdot \varepsilon_\lambda\}] \tag{5}$$

Where,
LST = Land Surface Temperature in °C
T_β = Sensor brightness temperature (°C)
$_\lambda$ = wavelength of emitted radiance
σ = Boltzmann Constant (1.38×10−23 J K−1)
h = Planck's Constant (6.626×10−34 J K−1)
C = Velocity of light (2.998 * 10-8 m s-1)

2.4.1 Urban Thermal Field Variance Index

Urban thermal field variance index (UTFVI) was used for the ecological evaluation of UHI in Abuja City. UTFVI is given by Eq. (6) (Guha et al., 2018).

$$UTFVI = \frac{T_s - T_m}{T_s} \tag{6}$$

Where,
UTFVI = Urban Thermal Field Variance Index
T_s = Land Surface Temperature (Kelvin)
T_m = Mean of Land Surface Temperature (Kelvin)

2.4.2 Urban Heat Island

The UHI assessment of heat stress is given by Eq. (7).

$$UHI = \frac{LST - LST_m}{SD} \quad (7)$$

Where,

UHI = Urban Heat Island
LST = Land Surface Temperature
SD = Standard Deviation

3. RESULTS

3.1 Land Cover Dynamics

The classified Landsat images of Abuja City for the year 1990, 2001, 2014 and 2020 are shown in (Figure 3). The images are ordered into five (5) land cover classes; agricultural land, bare-land, built-up, waterbody and vegetation. The land cover has shown progressions between 1990 and 2020 due urbanization.

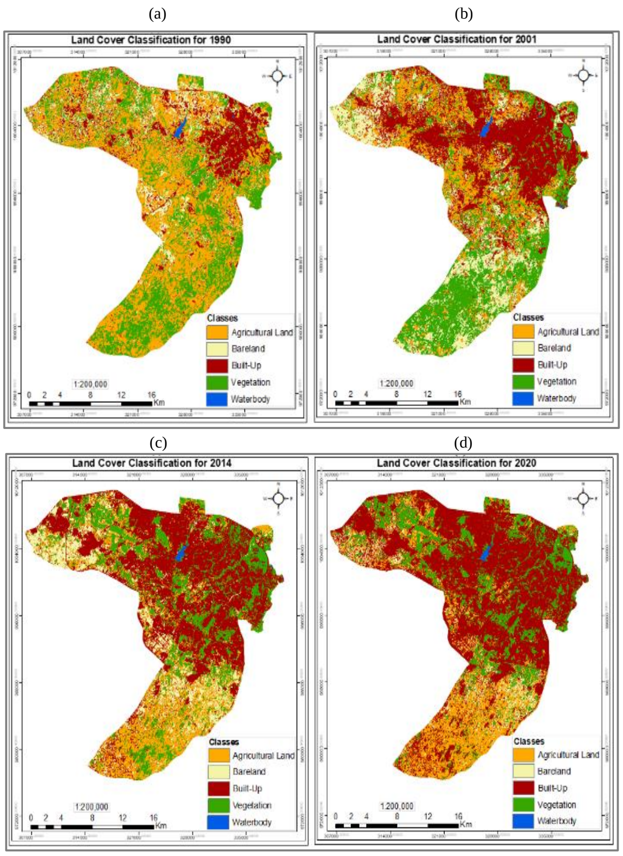

Figure 3: Land cover classification for Abuja City (a) 1990 (b) 2001 (c) 2014 (d) 2020

Table 2 shows the changes in land cover for 1990, 2001, 2014 and 2020 in Abuja City. Built-up area increased by 39.55% between 1990 and 2020, while agricultural land, vegetation, bare-land has decreased with 24.72%, 8.16% and 6.31% respectively. Waterbody showed a negligible change over the same period.

Land Cover	1990	2001	2014	2020
Waterbody	0.25	0.38	0.23	0.22
Bare-land	11.85	18.7	12.64	5.21
Built-up	15.9	34.93	44.55	55.45
Vegetation	27.45	26.77	21.59	19.29
Agricultural Land	44.55	19.22	20.99	19.83

Table 2: Percentage of land cover change from 1990 to 2020

3.1.1 Land Cover Transitions

The components of land cover transitions between 1990 to 2020 are presented in the order of loss, gain, total change, swap and net-change (Table 3). The result indicate that built-up area experienced the highest gain 44% and also the least loss at 4%. While, agricultural land experienced the highest loss at 34%. Then followed by vegetation that lost 21% and gained 13%. The highest change attributable to the absolute net gain was found in built-up areas (40%) and the least was found in bare-land (7%). Swap type of change was highest for vegetation, which has experienced nearly a pure swap of its total transition pattern.

Land Cover	Loss	Gain	Total Change	Swap	Net Change
Agricultural Land	34	9	43	19	-24
Bare-land	12	5	16	9	-7
Built-up	4	44	48	8	40
Vegetation	21	13	35	26	-8
Waterbody	0	0	0	0	0
Total	71	71	71	31	40

Table 3: Components of land cover transitions (1990-2020)

The proportion of each land cover category that remained static between 1990 and 2020 is presented as the diagonal values (Table 4). The results indicate that built-up has the highest persistence at 11.97%. Followed by agricultural land at 10.10%. While waterbody experienced the lowest persistence at 0.19%. An estimated 6.19% of vegetation persisted.

Land Cover		2020					
		Agricultural Land	Bare Land	Built-up	Vegetation	Waterbody	Total
1990	Agricultural Land	**10.10**	2.90	23.07	8.10	0.01	44.18
	Bare-land	1.32	**0.62**	7.90	2.32	0.01	12.16
	Built-up	0.78	0.40	**11.97**	2.79	0.00	15.92
	Vegetation	7.25	1.27	12.76	**6.19**	0.04	27.51
	Waterbody	0.00	0.00	0.00	0.04	**0.19**	0.23
Total		19.45	5.19	55.7	19.41	0.25	**100**

Table 4: Land cover transition matrix (1990-2020)

3.2 Land Surface Temperature Patterns

Figure 4 shows the distribution of Land Surface Temperature (LST) obtained from the Landsat scenes covering Abuja City for the year 1990, 2001, 2014 and 2020. The LST pattern reveals a significant anomaly between 1990 and 2020.

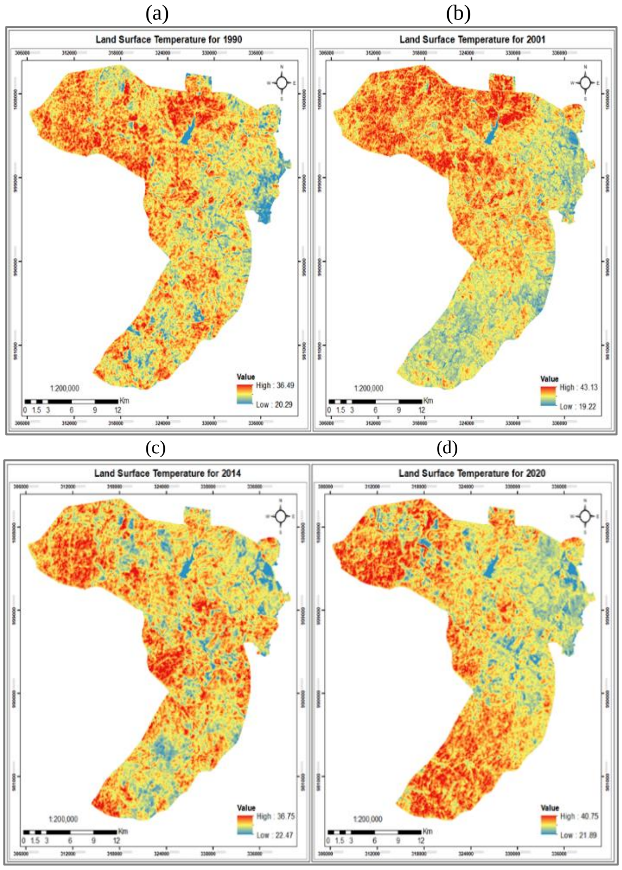

Figure 4: Land surface temperature distribution in Abuja City (a) 1990 (b) 2001 (c) 2014 (d) 2020

The minimum, maximum, standard Deviation and mean LST has shown a gradual increase between 1990 and 2020 (Table 5). The minimum LST ranged from 19°C to 23°C, while maximum LST ranged from 36°C to 43°C and mean LST ranged between 30°C to 34°C. The mean LST increased by 2.56 °C from 1990 to 2020. The result concur with (Mwangi et al., 2021; Oke, 1973).

	Land Surface Temperature (°C)				
Year	**Min**	**Max**	**SD**	**Mean**	**Mean Change**
1990	20.29	36. 75	1.48	31.23	0.00
2001	19.22	43.13	2.12	30. 75	0.45
2014	22.47	30. 49	1.42	30. 68	0.07
2020	21.89	40.75	1.76	33.24	2.56

Table 5: Descriptive analysis of land surface temperature

The mean thermal signature for each land cover type is shown in (Figure 5). Vegetation and water bodies exhibited the lowest mean LST, which can be attributed to their higher latent heat transfer and evapotranspiration (Ahmed et al., 2002). Highest mean LST was observed in agricultural land, bare-land and built-up areas. Bare-land reflects incoming radiation thereby warming up faster than other land cover types (Huang et al., 2015). These findings justify the dependence of LST on land cover types.

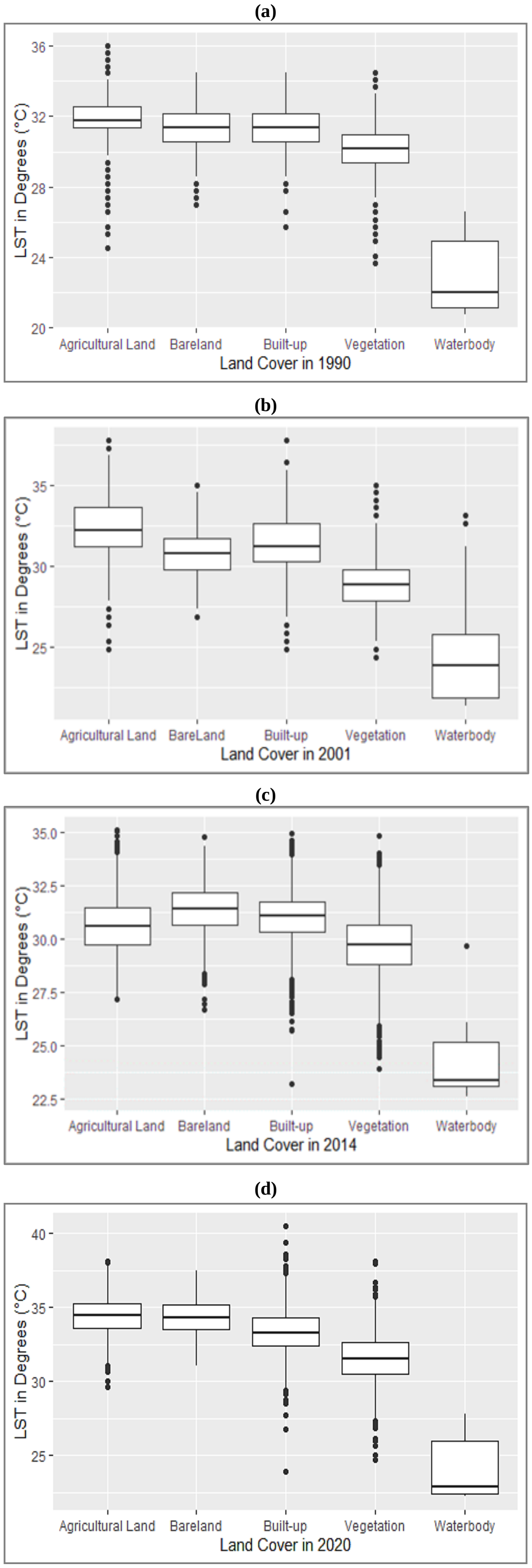

Figure 5: Thermal signature of land cover types (a) 1990 (b) 2001 (c) 2014 (d) 2020

https://doi.org/10.5194/isprs-archives-XLIII-B3-2022-699-2022

3.3 Evaluation of Thermal Comfort in Abuja city

The Urban Thermal Field Variance Index (UTFVI) was used to quantitatively describe the thresholds of thermal and ecological comfort in relation to Urban Heat Island (UHI) intensity in Abuja City (Figure 6). UHI intensity is extricable linked to anomalous changes in Land Surface Temperature (LST) (Alcantara et al., 2019). Built intensification alters surface energy budget (EPA, 2016), thereby decreasing the thermal comfort within cities.

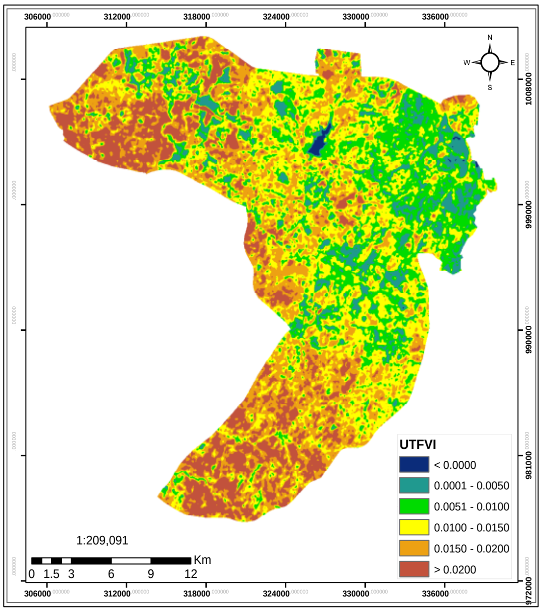

Figure 6: UTFVI for Abuja City

Table 6 summarizes the percentage coverage of UHI and EEI against the threshold of UTFVI. The results show that about 41.60% of the city's proportion experiences worst thermal condition (UTFVI > 0.02), while 42.90% experiences excellent thermal condition (UTFVI < 0.00). The sum of areas experiencing bad to worst thermal and ecological conditions is about 47.40% proportion of the city.

UTFVI	UHI	EEI	(%)
< 0.000	None	Excellent	42.9
0.000 - 0.005	Weak	Good	5.7
0.005 - 0.010	Middle	Normal	4.3
0.010 - 0.015	Strong	Bad	2.6
0.010 - 0.015	Stronger	Worse	3.2
> 0.020	Strongest	Worst	41.6

Table 6: Threshold of ecological evaluation index (EEI)

4. CONCLUSION

This paper analysed the spatial dimensions of land cover transitions and land surface temperature in Abuja city, Nigeria. Google Earth Engine (GEE) platform offers great potential in processing Landsat imagery to retrieve Land Surface Temperature (LST) and to classify land cover using Random Forest (RF) at high accuracy. The Landsat imageries were obtained during the dry season to avoid phenological variability between time points (Verbesselt et al., 2010). The analysis of transition matrix reveals that Abuja City has undergone significant change in land cover since its inauguration in 1990. Built-up is the dominant land cover that has significantly gained from the loss of other categories like vegetation, agricultural and bare-land. Built-up has also shown the highest level of persistence of changing to other land cover. The descriptive statistics of LST showed a significant increase in temperature from 1990 to 2020. Vegetation and water bodies recorded the lowest mean LST, which can be attributed to their higher latent heat transfer and evapotranspiration (Ahmed et al., 2002). Highest mean LST was observed in agricultural land, bare-land and built-up areas. Bare-land reflects incoming radiation thereby warming up faster than other land cover types (Huang et al., 2015). These findings justify the dependence of LST on land cover types. The urban thermal field variance index of Abuja City shows that a sizable portion of Abuja City is experience bad to worst thermal comfort. There is need for a proactive land management strategy that will contribute towards the achievement the goals of SDGs and improving the thermal comfort of urban dwellers.

REFERENCES

Abubakar, I.R., 2014. Abuja city profile. CITIES 41, 81–91. https://doi.org/10.1016/j.cities.2014.05.008

Adeyeri, O.E., Akinsanola, A.A., Ishola, K.A., 2017. Investigating surface urban heat island characteristics over Abuja, Nigeria: Relationship between land surface temperature and multiple vegetation indices. Remote Sens. Appl. Soc. Environ. 7, 57–68. https://doi.org/10.1016/j.rsase.2017.06.005

Adugna, A., Abegaz, A., Legass, A., Antille, D.L., 2017. Random and systematic land-cover transitions in north-eastern Wollega, Ethiopia. Bois Forets des Trop. 2, 3–15. https://doi.org/10.19182/bft2017.332.a31329

Ahmed, B.M., Hata, T., Tanakamaru, H., Abdelhadi, A.W., Tada, A., 2002. THE SPATIAL ANALYSIS OF SURFACE TEMPERATURE AND EVAPOTRANSPIRATION FOR SOME LAND USE / COVER TYPES IN THE GEZIRA 1–5.

Alcantara, C.A., Escoto, J.D., Blanco, A.C., Baloloy, A.B., Santos, J.A., Sta Ana, R.R., 2019. GEOSPATIAL ASSESSMENT and MODELING of URBAN HEAT ISLANDS in QUEZON CITY, PHILIPPINES USING OLS and GEOGRAPHICALLY WEIGHTED REGRESSION. Int. Arch. Photogramm. Remote Sens. Spat. Inf. Sci. - ISPRS Arch. 42, 85–92. https://doi.org/10.5194/isprs-archives-XLII-4-W16-85-2019

Braimoh, A.K., 2006. Random and systematic land-cover transitions in northern Ghana. Agric. Ecosyst. Environ. 113, 254–263. https://doi.org/10.1016/j.agee.2005.10.019

Cavan, G., Lindley, S., Jalayer, F., Yeshitela, K., Pauleit, S., Renner, F., Gill, S., Capuano, P., Nebebe, A., Woldegerima, T., Kibassa, D., Shemdoe, R., 2014. Urban morphological determinants of temperature regulating ecosystem services in two African cities. Ecol. Indic. 42, 43–57. https://doi.org/10.1016/j.ecolind.2014.01.025

Cetin, M., Musaoglu, N., Tanik, A., 2008. Multitemporal assessment of land-use change in a rapidly urbanizing coastal region in Turkey using remote sensing. Environ. Eng. Sci. 25, 917–928. https://doi.org/10.1089/ees.2006.0254

Dissanayake, D.M.S.L.B., Morimoto, T., Ranagalage, M., Murayama, Y., 2019. Land-use/land-cover changes and their impact on surface urban heat islands: Case study of Kandy City, Sri Lanka. Climate 7. https://doi.org/10.3390/cli7080099

Duan, H., Xie, Y., Du, T., Wang, X., 2021. Random and systematic change analysis in land use change at the

category level—A case study on Mu Us area of China. Sci. Total Environ. 777, 145920. https://doi.org/10.1016/j.scitotenv.2021.145920
EPA, 2016. Climate Change Indicators in the United States: Heat-Related Deaths 1–8.
Ermida, S.L., Soares, P., Mantas, V., Göttsche, F.M., Trigo, I.F., 2020. Google earth engine open-source code for land surface temperature estimation from the landsat series. Remote Sens. 12, 1–21. https://doi.org/10.3390/RS12091471
Guha, S., Govil, H., Dey, A., Gill, N., 2018. Analytical study of land surface temperature with NDVI and NDBI using Landsat 8 OLI and TIRS data in Florence and Naples city, Italy. Eur. J. Remote Sens. 51, 667–678. https://doi.org/10.1080/22797254.2018.1474494
Gumel, I.A., Aplin, P., Marston, C.G., Morley, J., 2020. Time-series satellite imagery demonstrates the progressive failure of a city master plan to control urbanization in Abuja, Nigeria. Remote Sens. 12. https://doi.org/10.3390/rs12071112
Hishe, H., Giday, K., Van Orshoven, J., Muys, B., Taheri, F., Azadi, H., Feng, L., Zamani, O., Mirzaei, M., Witlox, F., 2021. Analysis of Land Use Land Cover Dynamics and Driving Factors in Desa'a Forest in Northern Ethiopia. Land use policy 101. https://doi.org/10.1016/j.landusepol.2020.105039
Huang, W., Zeng, Y., Li, S., 2015. An analysis of urban expansion and its associated thermal characteristics using Landsat imagery. Geocarto Int. 30, 93–103. https://doi.org/10.1080/10106049.2014.965756
Leal Filho, W., Wolf, F., Castro-Díaz, R., Li, C., Ojeh, V.N., Gutiérrez, N., Nagy, G.J., Savić, S., Natenzon, C.E., Al-Amin, A.Q., Maruna, M., Bönecke, J., 2021. Addressing the urban heat islands effect: A cross-country assessment of the role of green infrastructure. Sustain. 13, 1–20. https://doi.org/10.3390/su13020753
Manakos, I., Gutman, G., Kalaitzidis, C., 2021. Monitoring land cover change: Towards sustainability. Land 10, 10–11. https://doi.org/10.3390/land10121356
Mccartney, S., Mehta, A., 2020. National Aeronautics and Space Administration Satellite Remote Sensing for Urban Heat Islands.
Mwangi, P W, Karanja, F.N., Kamau, P.K., Letema, S.C., 2021. Contribution index of land cover and land surface temperature changes in Upper Hill Nairobi, Kenya, in: ISPRS Annals of the Photogrammetry, Remote Sensing and Spatial Information Sciences. pp. 141–149. https://doi.org/10.5194/isprs-annals-V-3-2021-141-2021
Mwangi, P. W., Karanja, F.N., Kamau, P.K., Letema, S.C., 2021. Contribution index of land cover and land surface temperature changes in Upper Hill Nairobi, Kenya. ISPRS Ann. Photogramm. Remote Sens. Spat. Inf. Sci. 5, 141–149. https://doi.org/10.5194/isprs-annals-V-3-2021-141-2021
Oke, T.R., 1973. City size and the urban heat island. Atmos. Environ. 7, 769–779. https://doi.org/10.1016/0004-6981(73)90140-6
Pontius, R.G., Shusas, E., McEachern, M., 2004. Detecting important categorical land changes while accounting for persistence. Agric. Ecosyst. Environ. 101, 251–268. https://doi.org/10.1016/j.agee.2003.09.008
Talukdar, S., Singha, P., Mahato, S., Shahfahad, Pal, S., Liou, Y.A., Rahman, A., 2020. Land-use land-cover classification by machine learning classifiers for satellite observations-A review. Remote Sens. 12. https://doi.org/10.3390/rs12071135
UN-DESA, 2019. World Urbanization Prospects, World Urbanization Prospects: The 2018 Revision (ST/ESA/SER.A/420).
UN-Habitat, 2020. The new urban agenda. https://doi.org/10.18356/4665f6fb-en
UNCCD, 2017. Global Land Outlook: Secretariat of the United Nations Convention to Combat Desertification.
United Nations Urban Settlement Programme, 2019. World population prospects 2019, Department of Economic and Social Affairs. World Population Prospects 2019.
Verbesselt, J., Hyndman, R., Zeileis, A., Culvenor, D., 2010. Phenological change detection while accounting for abrupt and gradual trends in satellite image time series. Remote Sens. Environ. 114, 2970–2980. https://doi.org/10.1016/j.rse.2010.08.003

ACKNOWLEDGEMENTS

The authors would like to acknowledge the German Academic Exchange Service (DAAD) for funding the 1st author.